

<sup>1</sup> Hussein Abdulqader  
Hussein

<sup>2</sup> Sameer Abdulstar  
Lafta

<sup>3</sup> Noaman Ahmed  
Yaseen AL-Falahi

<sup>4</sup> Mohanad Mahdi  
Abdulkareem

## The Detection and Classification from the Multimodal Images using Artificial Intelligence for Lung Diseases



**Abstract:** - Lung cancer is a disease in which healthy cells in the body gradually convert into tumour cells, resulting in a variety of medical issues. A standard dataset exists for lung cancer. With the rising incidence of lung cancer and the exponential growth of CT pictures, having a quick and effective way to evaluate CT scans can help physicians or surgeons develop an early treatment plan. In this research, two approaches are investigated for lung cancer prediction. One approach is based on training machine learning model on the features extracted from image processing techniques. And the other approach involves Artificial Intelligence models for lung cancer detection. Computed Tomography (CT) pictures are useful for determining the stage of lung cancer in a patient. As a result, CT images of the lung region are explored in this study by constructing a content-based image retrieval system using various machine learning and Artificial Intelligence techniques. For medical photos, texture analysis is critical. As a result, algorithms such as the K-Means clustering method and morphological operations such as erosion, dilation, and so on are used

**Keywords:** Lung cancer, multimodal images, Artificial intelligence Machine learning Optimization

### I. INTRODUCTION

Pneumonia is the leading cause of death in children all around the world. Every year, over 1.4 billion kids suffer from pneumonia, accounting for 18% of all children under the age of 5. Every year, pneumonia affects two billion individuals around the world. Pneumonia was an infection of the lungs that can be induced by viruses and bacteria. Fortunately, antibiotics and antiviral medicines can effectively treat this bacterial or viral infection. Nonetheless, quicker identification of bacterial or viral pneumonia and subsequent administration of the appropriate treatment can considerably reduce the risk of the patient's condition deteriorating and eventually leading to death. X-rays of the chest are now the most effective means of diagnosing pneumonia. Because the X-ray images of pneumonia are not always clear, these are frequently misidentified as other illnesses or benign anomalies. Furthermore, specialists may misclassify viral or bacterial pneumonia photos, resulting in patients receiving incorrect medicine and, as a result, worsening their condition. There have been reports of significant subjective variations in radiologists' decisions while detecting pneumonia. In low-resource countries (LRCs), there is also a scarcity of skilled radiologists, particularly in rural regions. As a result, there is a compelling demand for CAD systems that can assist radiologists in quickly recognizing distinct kinds of influenza from chest X-ray pictures [1].

Cancer is a serious disease that attacks and transforms healthy cells into cancerous ones. The lung is the most cancer-prone part of the body. As a result, many people around the world are prone to lung cancer, and the WHO keeps track of deaths. In 2018, there were 1.76 million deaths and 2.09 million cases, as per the WHO. Because early identification of lung cancer is challenging, different computer-assisted diagnostic approaches have been developed to aid doctors in identifying concerning lung nodules [2]. A range of imaging modalities, such as CT, MRI, and X-ray, can be used to identify lung cancer. Due to decreased distortion and noise, the CT scan captures the features seen in distinct areas of the Lungs better than any other imaging modality, allowing radiologists to

<sup>1</sup>\*Corresponding author: Middle Technical University, Technical Instructors Training Institute, Baghdad, Iraq

<sup>2</sup>Middle Technical University, Technical Instructors Training Institute, Baghdad, Iraq

<sup>3</sup>Director of Data Centers Management Department, Assistant chief engineer, Iraqi Ministry of Communications, Baghdad-Iraq

<sup>4</sup>Digital Transformation Department, Senior Chief of Programmers, Iraqi Ministry of Communications, Baghdad, Iraq

grasp and identify the occurrence of sickness. As a result, CT scans were used to perform the investigation in this research [3].

Even though lung cancer is relatively widespread, it is feasible to increase the rate of survival from 14% to 49%. While evaluating CT images from patient information may help enhance patient efficacy and therapy, it is a time-consuming and complicated process. Rather than evaluating each image separately, radiologists can gain additional information by identifying a picture from the database that is a close match to the image database. The recovery of relevant photographs from a large database is a relatively new subject of study. The CBIR algorithm is presented to make it easier to retrieve photos based on their properties. The purpose of this study is to compare two deep neural networks and determine which architecture helps the most to close the semantic difference and enable the development of a more efficient CBIR system for CT scan images of lung cancer [4].

Lung cancer has been one of the leading causes of mortality around the globe. It is critical to be able to identify the type of tumour as well as forecast patient clinical results. Lung cancer sufferers have a lower standard of living than the general population and patients with other cancers. If lung cancer is detected early, at least 50 % of patients will still be alive 5 years later, free of recurrence. Normal cells acquire a metamorphosis that leads them to develop abnormally, reproduce without control, and ultimately spread to other areas of the body, resulting in cancer. The cells combine to produce a mass or tumour that is distinct from the organs from which it arose [5].

The human body consists of billions of single cells, most of which produce new cells to replace older cells that have matured or become destroyed. This well-ordered procedure of exclusively producing new cells while a person is growing can occasionally fail. When this occurs, cells can become uncontrollably proliferate and create a mass or lump known as a tumour (Cancer). The categorization of lung glandular tissue as benign or malignant (Cancer Cells) is handled in this method. An automated platform is established after obtaining the necessary data concerning the info of lung disease, methods obtainable for diagnosis of lung cancer, testing methods for lung disease, different types of lung cancer, info of sputum tissue samples, and how the picture is collected from sputum cytology images [6].

There are various options for individuals with cough, haematuria, or heart palpitations who have radiologic anomalies, whether or not they are symptomatic of lung cancer. CT scans, both standard and high-resolution, can help to explain the nature of a worrisome lesion or reduce the diagnostic options. It has been stated that a more precise diagnosis needs morphologic depth analysis using cytological methods or biopsy. The most common methods for diagnosis include cytological investigation of sputum, lung secretions. Sputum histology is the oldest and most basic of these diagnostic tests, and it is widely available to all medical professionals. It can diagnose the most basic lung carcinomas, based on the nature and stage of the tumour. Sputum histology may also provide a platform for searching for lung cancer- detecting molecular indicators [7].

It is critical to identify lung cancer at an earlier stage to reduce fatality rates. Only mass testing of all males with a greater than average incidence of lung cancer can achieve this. Lung cancer has been detected using a combination of chest X-ray and sputum investigation as a screening tool. However, it was not found to be useful. To identify early lung malignancies and their precursor tumours, imaging methods coupled with sputum cytology will be extremely useful. To screen all qualified people in the area, a large number of resources and manpower may be required. Sputum specimens may require a significant number of qualified cytologists for microscopic examination. If a low-cost computer-assisted microscopic examination of sputum cytology smears could be created, it will greatly aid the implementation of a universal lung cancer monitoring program [8].

Artificial Intelligence enables simulation approaches with several processing elements to acquire multiple degrees of abstraction for data models. The data has become large data as a result of remarkable advancements in image capturing technologies, making image analysis difficult. This rapid expansion of medical pictures and modalities necessitates enormous efforts by medical experts, which are subjective, susceptible to human inaccuracy, and may vary significantly amongst experts. Traditional methods are insufficient to deal with medical huge data, so an Artificial Intelligence-based automatic diagnostic system is deployed. Artificial Intelligence is a collection of machine learning methods that use deep architectures made up of numerous non-linear changes to represent high-level concepts in data. Artificial Intelligence is designed to work like the nervous system, with a deep model that mimics how data is processed in the brain through numerous layers of modification [9].

To retrieve the most relevant attributes from a data gathering, a strong understanding of the underlying properties is needed. When a large amount of data needs to be processed quickly, this can become laborious and complex. Artificial Intelligence approaches have the potential to immediately learn feature models by enabling the system to acquire complicated features from raw photos, which is a significant advantage [31,32]. This enables us to create a system that isn't reliant on hand-crafted characteristics, which are typically necessary for other machine learning approaches. When compared to standard methods without training, Artificial Intelligence methods are recognized for the concise extraction of data from medical pictures and have been shown to enhance efficiency. These characteristics have sparked interest in studying the advantages of Artificial Intelligence in medical picture processing. Artificial Intelligence methods have advanced to the point that they are now seen as critical factor in future healthcare applications [10]. This study is arranged as follows: in part 2, a description of the literature review; in section 3, a description of the research technique; in section 4, an analysis of the results and discussion; and in section 5, a description of the final conclusion and future work.

## 1. LITERATURE REVIEW

Literature review in respect to Study of Lung Diseases Detection and Classification from the Multimodal Images using Artificial Intelligence.

Prioritizing Circ RNA-disease relationships with a convolutional neural network based on multiple similarity feature fusion is proposed by [11].

In [12] suggests using a single neural network to predict ratings. The DT-diaphoreses activity and messenger RNA content in human non-small cell lung carcinoma: connection to the responsiveness of lung tumourxenografts to mitomycin.

In [13] introduced the Three-dimensional CNN architecture to provide a radiological evaluation of spinal lumbar MRIs and also pinpoint the expected diseases utilizing intervertebral disc sizes.

In [14] presented a scalable Internet of Things device for heart disease diagnostics. The detected data from the Internet of Things device was processed using the logistic regression approach. The vast volume of data acquired from patients was stored and retrieved via cloud services. ROC analysis was used to assess the efficiency of the regression models in predicting heart disease.

In [15] used boundary data and algorithms including the Gabor filter, Markov chain, and Haralick to extract textural properties from lung cancer CT images. The proposed system was dubbed 'BRISC.' The system's performance was tested using 2424 photographs, and it was found to be 88 percent accurate.

To determine pair wise similarity, [16] used lexical and perceptual similarity retrieval as well as weighted network creation. The quickest route is constructed graphs return photos that are similar to the search picture. Using HOG and multi-resolution retrieval, SVM categorization, and cosine image similarity, data was extracted at a range of levels, namely minimal, meaningful, and situational, from the LISS dataset. Given CNN architectures' improved performance, we compared the performance of two different CNN models in the CBIR method in this study.

In [17] proposed a lobe fissure tracking system based on a redesigned optimization technique. The region edges are enhanced using the Robinson and Kirsch filters. The intensity of lobe fissure is determined using Otsu's approach. The Robinson & kirsch filters are used to improve the image. The ant colony method is a method for detecting.

In [18] scanned them adaptively in a sagittal view. For the first segmentation of lung regions, region growth is used. A line improvement filter based on a Hessian matrix is used, followed by a uniform cost filter.

Landslide fissure modeling for multi-scale edge detection was described by [19]. The linear dark curving characteristics are removed. The cracks are detected using a Gaussian matched filter that combines the first component of a Gaussian filter.

In [20] stated that they used a sweeping technique to determine the fissure location at first. Finally, wavelet analysis was employed to locate fissure locations and corrugations in the fissure region.

Medical images are influenced by many types of sounds, which are removed using the filtering approach, according to the literature review. In [21] show threshold-based segmentation. GLCM was used to extract textural and architectural features from fundus images; however, feature extraction takes longer.

Poor contrast quality and noise are two of the most typical flaws in medical photographs. In

[22] developed a morphological transformation technique for improving contrast and quality in medical data.

The medical picture is more precise and clear visual data in the created image to clinical diagnosis as the detailed info increases. The resulting images have superior results to the original medical photographs, and the procedure is easy and efficient [23].

In [24] Ensemble learning is models that are made up of numerous weaker models that are learned separately and then integrated in some way to create a final prediction.

Segmentation techniques, which also included skull stripping and morphological operations for pre-processing, were used to classify brain tumours using neural networks [25]. The wavelet transforms were used to decompose and extract features from an MR image. Finally, AdaBoost classification techniques were utilized to identify discriminative characteristics from MRI images to classify them as cancerous or benign. AdaBoost classifier was created by smoothing the images utilizing partial differential models. In this case, the algorithm was less accurate.

In [26] Medical image categorization study has yielded numerous study outcomes and was implemented clinically. Machine learning doesn't really necessitate any healthcare expert knowledge, nor does it necessitate engineering tech features. This may acquire key qualities like colour and edge using the first layer, and then utilize the underlying surface to learn more complex features of lung imaging data sets.

In [27] suggested three EANNs and DoG for the categorization of micro-calcification clusters in mammograms. They compared their suggested strategy to a back propagation-trained feed-forward Neural Network (NN).

In [28] Using helical CT scans, they established a CAD method for disease diagnosis. This strategy can reduce time complexity while increasing diagnosis confidence. This procedure consists of two stages: analysis and diagnosis. The lung and pulmonary blood vessel area will be removed, and its characteristics will be analyzed using the image processing method in the analysis step. These characteristics, as well as the tumour's location, were used to develop the diagnostic rule.

In [29] give computer-aided diagnostics for lung CT utilizing artificial life models. Several strategies in the CAD system, centre of maximal balls, include region growing, form models, and active counter, but it is thought that the biological simulations of ants, also known as artificial life models, are at the heart of this method. The image's ribcage is first recognized using a 3D region expanding method. The active contour is then employed to create the limited area around the ribs, and it is set up to restore the vascular and bronchial tree flawlessly and cleanly.

In [30] suggested a novel CAD method for early lung nodule detection. The volumetric variations in the detected lesion over time are used to calculate the growth rate of the identified lung nodule. This method's process is divided into five phases. The first step is to divide the lung area on the CT scan and then locate the lung nodule within the segmentation process.

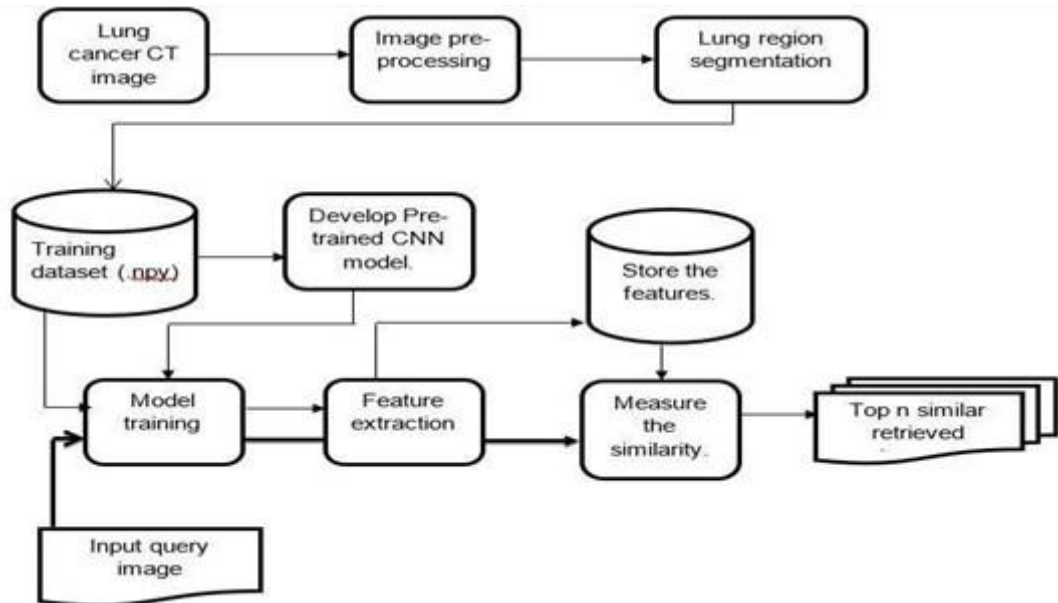
## 2. RESEARCH METHODOLOGY

Deep learning models retrieve more significant properties than traditional machine learning approaches. The models are examined in this section to locate a suitable model for constructing the CBIR system. For the specified hyper parameters, the VGG16 model surpasses the others. The KNN approach is used to process the extracted features by training the VGG16 network on the pre-processed input photos to find closely related pictures from the collection to the source images query.

### 3.1. METHODOLOGY

The proposed framework is built in stages. Image processing techniques such as a median filter, anisotropic filter, morphological operations, and K-means clustering are used to enhance training images and segment only the lung region from lung cancer CT images. Following the extraction of the region of interest, two pre-trained models – VGG16 and ResNet – were created, each using two separate optimizers Adam and RMS prop [31-33].

The segmented lung image is fed into and educated by deep learning models. VGG16 was discovered to perform better. As a result, the final entirely linked layers of VGG16's final layer are retrieved. All of the preceding processes are also applied to the input query image. The KNN algorithm is fed both the feature vector of the training and query photos, and the top nearest images are obtained. Figure 1 depicts the foundation for the CBIR system developed in this study, followed by Algorithm 1, which outlines the operations.



II. FIGURE 1: PROPOSED CBIR FRAMEWORK ALGORITHM 1: DEEP LEARNING-BASED CBIR SYSTEM

1. Acquisition of a lung cancer picture collection from the LIDC database
2. Utilize the pylidc package to convert Dicom pictures to .npy.
3. Denoising and image enhancement methods are used to pre-process the greyscale information.
4. By stacking the one-dimensional channel three times, you may enlarge the one-dimensional greyscale image to three channels in size (224, 224).
5. Create and build VGG16 and ResNet pre-trained CNN architectures
6. Compile CNN architectures are developed
7. Using stratified sampling, divide the dataset into training, test, and validation subsets in a 60-20-20 ratio.
8. Utilize pre-processed training data to train the pre-trained Artificial Intelligence model, verify it using the validation dataset, and evaluate it using test data.
9. Using the Adam and RMSprop optimizers, repeat steps 6 and 7.
10. Measure a model's accuracy, recall, and F1 score. Additionally, select the highest-scoring VGG16 model.
11. Extract the features from the flatten layer of the VGG16 model.

12. Utilize the produced architectures to forecast the characteristics of test input.
13. Calculate the Euclidean and Manhattan distances between the attributes of the testinput and those of the database images.
14. Conduct analysis and comparison of the output.

### 3.2. DATA ACQUISITION

The deep learning models in this work are trained using the LIDC/IDRI database. There are 1088 CT scan images in the collection, as well as a CSV file with patient information. A specific number of CT imaging slices is given to each patient. The CT image slices were read into Dicom format using the pylidc program. The complete distribution of CT slice photographs with true or fake cancer cases is presented in Figure 2 after filtering the excel file's 'is clean' column property. In addition, database samples are shown in Figure 3.

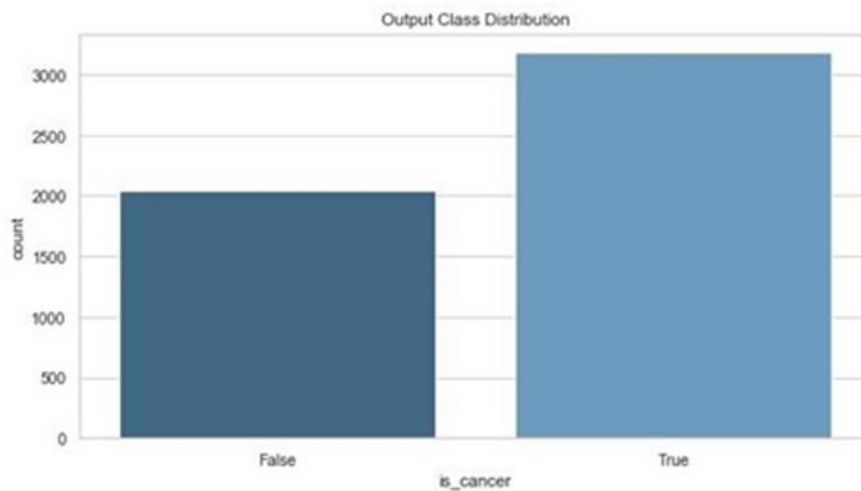


FIGURE 2: LIDC/IDRI OUTPUT CLASS DISTRIBUTION

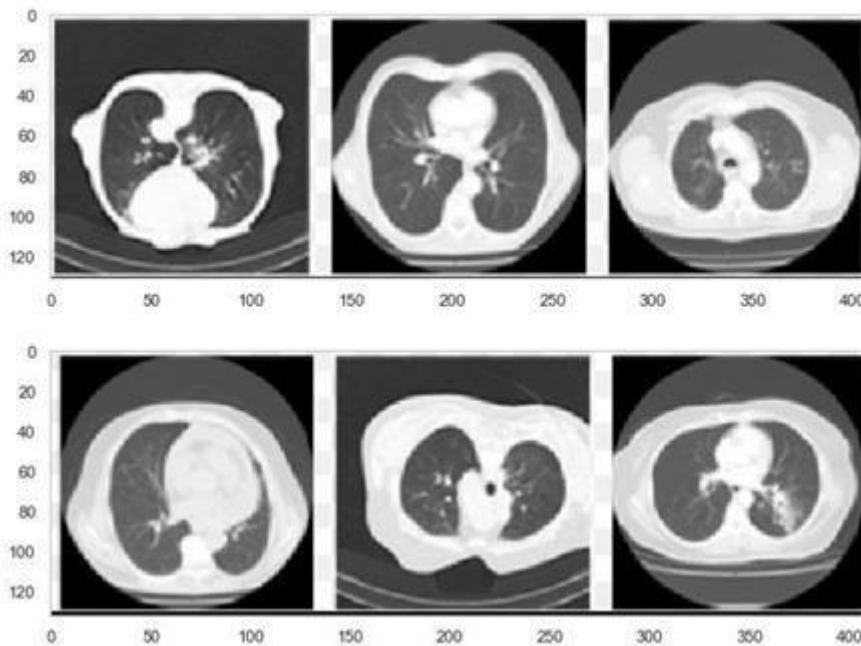


Figure 3: Sample Lung CT Images

### 3.3. DATA PRE-PROCESSING AND SEGMENTATION

Image augmentation with the median filter and picture Denoising with anisotropic diffusion is included in the pre-processing of the collected photos. Anisotropic diffusion reduces noise while preserving significant sections of a picture. The lung region is segmented using morphological erosion, dilation, and K-means clustering to build a mask from the improved pictures. The designed mask aids in the segmentation of the lungs. The following section summarises each operation as algorithm 2.

III. ALGORITHM 2: PRE-PROCESSING AND SEGMENTATION OF LUNG REGIONS

1. Analyze the CT images of lung cancer that were provided as input.
2. Normalize the values of the pixels
3. Utilize a median filter with a three-dimensional kernel.
4. Apply an anisotropic filter to eliminate noise from the picture while preserving thenodule border.
5. Conduct K-means clustering
6. Create a mask for the lung area by eroding and dilating the morphology.
7. Repeat the morphological dilation technique until the inner and exterior portions ofthe lung mask are filled.
8. To acquire the desired lung area, multiply the mask by the original image.

Table 1 summarises the multiple parameters and hyper parameters connected with the various layer types present in the Artificial Intelligence model.

IV. TABLE 1: PARAMETERS AND HYPER PARAMETERS OF ARTIFICIAL INTELLIGENCE

Layers	Parameters	Hyper parameters
Convolution	Kernels	Kernel size and number, activation function, stride, and padding values are all variables toconsider.
Pooling	None	Stride and padding values, pooling mechanism, and filter size are all factors to consider.
Fully connected	Weights	Number of weights and activation function
Others		The type of loss function, regularisation, and optimizer used in the model, as well as the value of learning rate and epoch, weight initialization minibatch, and dataset splitting.

3.4. Network Training

Gray-scale images are used to divide the images. The characteristics in this study were extracted using pre-trained VGG16 and ResNet50 deep learning models. Grayscale images were layered to provide a three-channel input due to the network's three-channel input structure. The pre-trained model was enhanced with additional flattening and dense layers,

and also a final layer with sigmoid activation function while maintaining the trainable state for the last few layers. 3918 data points were sampled due to memory limits. The sampled data were divided into sixty percent for training, twenty percent for validation, and twenty percent for testing, as shown in Figure 4. The flattened layer's features were extracted after the model was trained on the provided data.

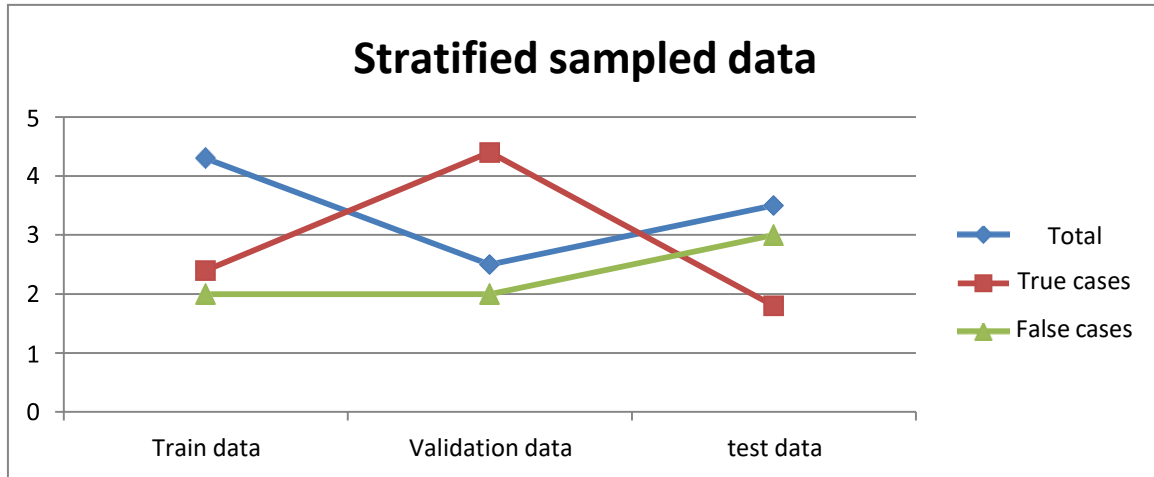


FIGURE 4: SAMPLED DATA

#### 4. Results & discussion

The experiment is developed entirely in Python, and it makes use of the Keras framework. Throughout this inquiry, accuracy, precision, recall, and the f1 score were all employed at different stages to determine the best technique. Accuracy was tested to see which deep learning model performed best and to choose the best model for the planned CBIR system. Precision and recall are used to evaluate the efficacy of a proposed technique.

V. TABLE 2: AVERAGE ERROR RATE AND AVERAGE COMPUTATION TIME

Iterations	Average error rate			Average consumption time (sec)		
	Precision	Recall	False positive	F-Measure	MissRate	False negative
10	0.5375	0.4	0.35	0.018162	0.012237	0.014621
20	0.4	0.35	0.275	0.019874	0.014943	0.010203
30	0.3875	0.325	0.3	0.021312	0.011617	0.013204
40	0.375	0.3	0.325	0.022683	0.010491	0.014435
50	0.375	0.3	0.3	0.023986	0.01065	0.010167

Table 3 Error rate deviation and computation time deviation

Iterations	Error rate deviation	Computation time deviation(sec)
------------	----------------------	---------------------------------



	Precision	Recall	False positive	F-Measure	MissRate	False negative
10	0.158607	0.229129	0.122474	0.004236	0.00342	0.006892
20	0.122474	0.122474	0.075	0.001454	0.009629	0.000887
30	0.117925	0.114564	0.1	0.002176	0.003505	0.008579
40	0.136931	0.1	0.114564	0.003372	0.000816	0.011351
50	0.125	0.1	0.1	0.004663	0.000629	0.001296

True positive, true negative, false positive, false negative, precision, and recall are denoted by the abbreviations TP, TN, FP, FN, P, and R. The ratio of relevant counted photos to total counted images is referred to as precision. The recall is defined as the proportion of relevant photos recovered to the total number of relevant images in the database. The samples from the segmented lung area are shown in Figure 5. The results of training ResNet and VGG16 with two different optimizers.

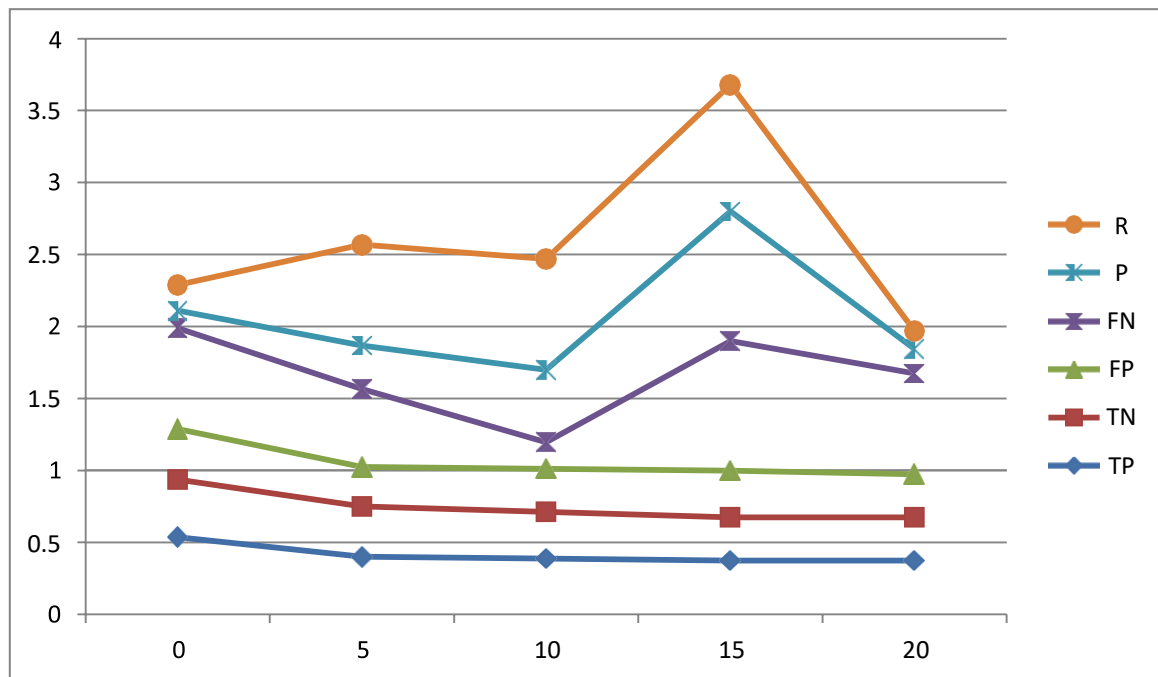
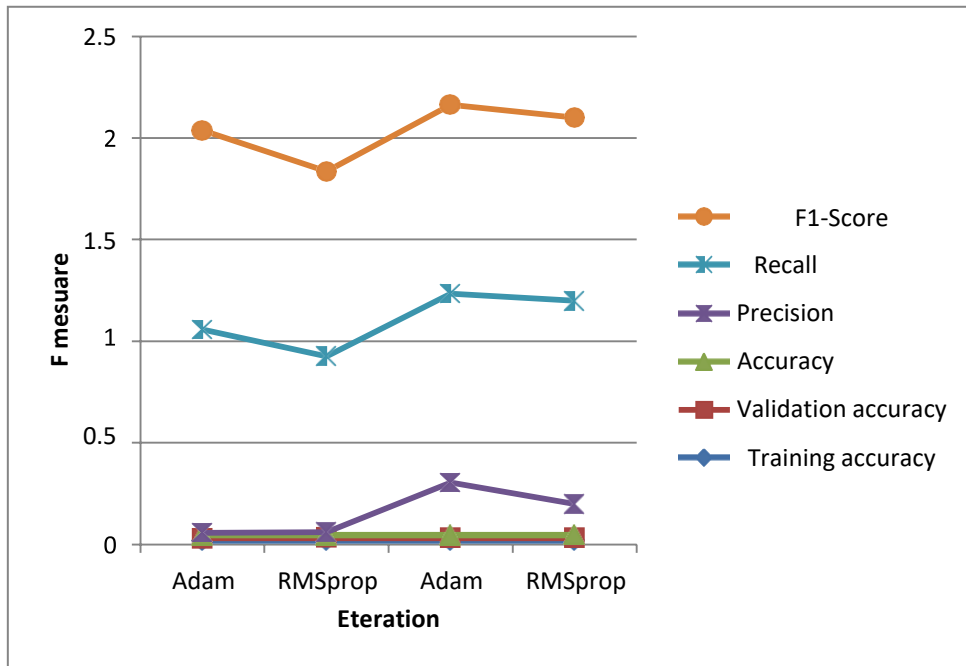


Figure 5: Analysis of optimum 'K' value using F-Measure

K is determined by experimenting with various test cases such as TP, TN, FP, FN, P, and R... Experiments are conducted using both samples of AOL and MCET datasets. Average F- Measure is analyzed to find the optimum value of K and presented in Figure 5



VI. FIGURE 6: VGG16 AND RESNET50 RESULTS

Adam and RMSprop – are summarised in Figure 6. The VGG16 with Adam optimizer performs better, as indicated by the greatest F1-score in Figure 6. As a result, the VGG16 model with Adam optimizer is utilized for feature extraction.

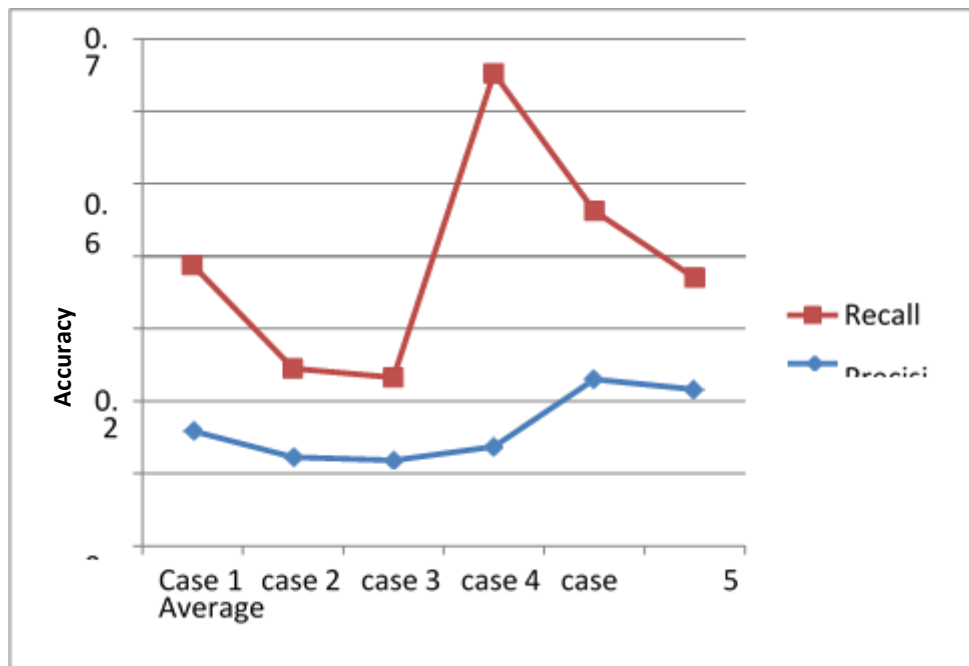


FIGURE 7: RESULT OF KNN ALGORITHM FOR DIFFERENT CASES

The flattened layer's attributes are extracted. Each train and test data set's unique properties are extracted and utilized to train the KNN model. Figure 7 outline the output of KNN model's for various cases.

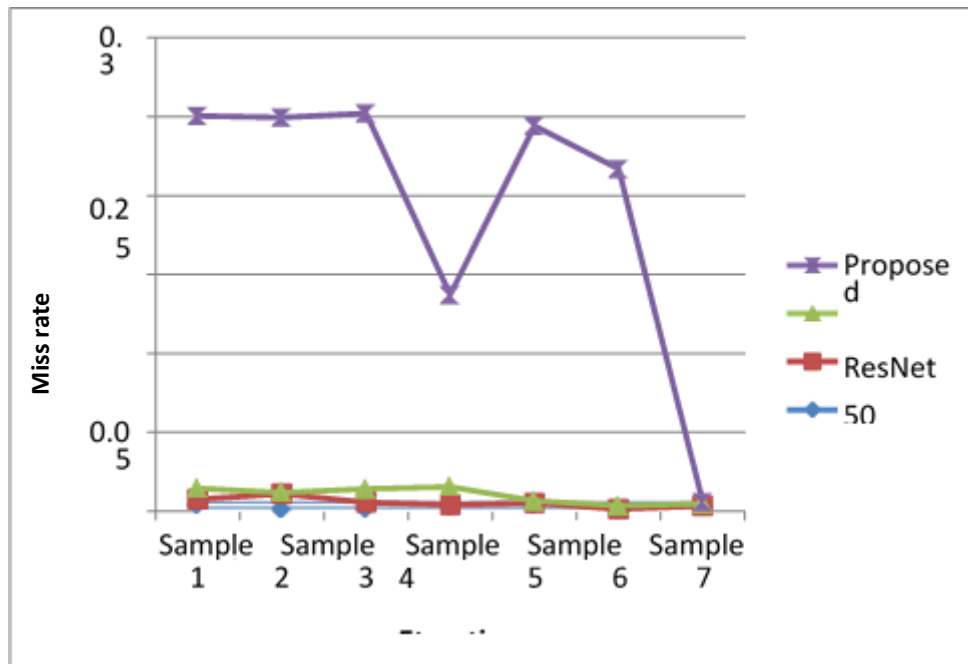


FIGURE 8: MISS RATE ANALYSIS OF VARIOUS PROPOSED ALGORITHMS

MR results are visualized in Figure 6 respectively. Negligible MR and FR reduction have been found to be achieved by VGG16 and ResNet50 algorithms. Analysis of Matthews Correlation (MC) is also examined to verify the performance of proposed algorithms.

## 5. CONCLUSION & FUTURE WORK

Each year, CT scan images of lung cancer increase considerably. By assisting radiologists in the development of a CBIR system capable of locating the top results that are the most comparable to the input image database, different key insights will be gained that will aid in the improvement of patient care. The LIDC dataset is obtained, pre-processed, and segmented to train and choose pre-trained deep learning models (VGG16 and ResNet50) with superior feature sets. Due to the superior performance of the VGG16 with Adam optimizer, the recovered features are fed into the KNN model during training. The findings indicate that the characteristics derived from the deep learning model point in the direction of developing an efficient CBIR system. This study will be extended in the future by training on a real-time dataset. Additionally, we will examine the features extracted from VGG16 using a variety of deep learning models, such as auto encoders, deep belief networks, and others, as well as various hyper parameter tuning techniques, to determine the efficiency with which characteristics can be recovered to develop a CBIR system suitable for real-world practices.

## REFERENCES

- [1] Boudria, A, AbouFaycal, C, Jia, T, Gout, S, Keramidas, M, Didier, C, Lemaitre, N, Manet, S, Coll, J-L & Toffart, A-C 2019, 'VEGF 165 b, a splice variant of VEGF-A, promotes lung tumor progression and escape from anti-angiogenic therapies through a  $\beta 1$  integrin/VEGFR autocrine loop', *Oncogene*, vol. 38, no. 7, pp. 1050-1066.
- [2] Boysen, G, Jamshidi-Parsian, A, Davis, MA, Siegel, ER, Simecka, CM, Kore, RA, Dings, RP & Griffin, RJ 2019, 'Glutaminase inhibitor CB-839 increases radiation sensitivity of lung tumor cells and human lung tumor xenografts in mice', *International journal of radiation biology*, vol. 95, no. 4, pp. 436-442.
- [3] Du, Q, Baine, M, Bavitz, K, McAllister, J, Liang, X, Yu, H, Ryckman, J, Yu, L, Jiang, H & Zhou, S 2019, 'Radiomic feature stability across 4D respiratory phases and its impact on lung tumor prognosis prediction', *Plos one*, vol. 14, no. 5, p. e0216480.
- [4] Eichner, LJ, Brun, SN, Herzig, S, Young, NP, Curtis, SD, Shackelford, DB, Shokhirev, MN, Leblanc, M, Vera, LI & Hutchins, A 2019, 'Genetic analysis reveals AMPK is required to support tumor growth in murine Kras-dependent lung cancer models', *Cell metabolism*, vol. 29, no. 2, pp. 285-302. e287.
- [5] El-Regaily, SA, Salem, MA, Abdel Aziz, MH & Roushdy, MI 2018, 'Survey of computer aided detection systems for

- lung cancer in computed tomography', *Current Medical Imaging*, vol. 14, no. 1, pp. 3-18.
- [6] Flatten, V, Baumann, K-S, Weber, U, Engenhart-Cabillic, R & Zink, K 2019, 'Quantification of the dependencies of the Bragg peak degradation due to lung tissue in proton therapy on a CT-based lung tumor phantom', *Physics in Medicine & Biology*, vol. 64, no. 15, p. 155005.
  - [7] Gang, P, Zhen, W, Zeng, W, Gordienko, Y, Kochura, Y, Alienin, O, Rokovyi, O & Stirenko, S 2018, 'Dimensionality reduction in deep learning for chest X-ray analysis of lung cancer', in 2018 tenth international conference on advanced computational intelligence (ICACI), pp. 878-883.
  - [8] Geetharamani, G & Pandian, A 2019, 'Identification of plant leaf diseases using a nine-layer deep convolutional neural network', *Computers & Electrical Engineering*, vol. 76, pp. 323-338.
  - [9] Hung, W-T, Hung, M-H, Wang, M-L, Cheng, Y-J, Hsu, H-H & Chen, J-S 2019, 'Nonintubated thoracoscopic surgery for lung tumor: seven years' experience with 1,025 patients', *The Annals of thoracic surgery*, vol. 107, no. 6, pp. 1607-1612.
  - [10] Jiang, J, Hu, YC, Tyagi, N, Zhang, P, Rimner, A, Deasy, JO & Veeraraghavan, H 2019, 'Cross modality (CT MRI) prior augmented deep learning for robust lung tumor segmentation from small MR datasets', *Medical physics*, vol. 46, no. 10, pp. 4392-4404.
  - [11] Fan, C, Lei, X & Pan, Y 2020, 'Prioritizing CircRNA-disease associations with convolutional neural network based on multiple similarity feature fusion', *Frontiers in genetics*, vol. 11, p. 1042.
  - [12] Maghari, AM, Al-Najjar, IA, Al-Laqtah, SJ & Abu-Naser, SS 2020, 'Books' Rating Prediction Using Just Neural Network', *International Journal of Engineering and Information Systems (IJEAIS)*, vol. 4, no. 10.
  - [13] Chen, H, Jiang, Y, Ko, H & Loew, M 2021, 'A Teacher-Student Framework with Fourier Augmentation for COVID-19 Infection Segmentation in CT Images', arXiv preprint arXiv:2110.06411.
  - [14] Conde, J, Tian, F, Hernández, Y, Bao, C, Cui, D, Janssen, K-P, Ibarra, MR, Baptista, PV, Stoeger, T & Jesús, M 2020, 'In vivo tumor targeting via nanoparticle-mediated therapeutic siRNA coupled to inflammatory response in lung cancer mouse models', *Biomaterials*, vol. 34, no. 31, pp. 7744-7753.
  - [15] Cristin, R, Kumar, BS, Priya, C & Karthick, K 2020, 'Deep neural network based Rider-Cuckoo Search Algorithm for plant disease detection', *Artificial intelligence review*, vol. 53, no. 7.
  - [16] Simsek, M, Obinikpo, AA & Kantarci, B 2020, 'Deep learning in smart health: methodologies, applications, challenges', in *Connected Health in Smart Cities*, Springer, pp. 23-46.
  - [17] Huang, C-J, Chen, Y-H, Ma, Y & Kuo, P-H 2020, 'Multiple-input deep convolutional neural network model for covid-19 forecasting in china', *MedRxiv*.
  - [18] El-Mahelawi, JK, Abu-Daqah, JU, Abu-Latifa, RI, Abu-Nasser, BS & Abu-Naser, SS 2020, 'Tumor Classification Using Artificial Neural Networks', *International Journal of Academic Engineering*, vol. 4, no. 11.
  - [19] Fan, C, Lei, X & Pan, Y 2020, 'Prioritizing CircRNA-disease associations with convolutional neural network based on multiple similarity feature fusion', *Frontiers in genetics*, vol. 11, p. 1042.
  - [20] Ghazaly, NM, Abdel-Fattah, MA & El-Aziz, A 2020, 'Novel coronavirus forecasting model using nonlinear autoregressive artificial neural network', *International Journal of Advanced Science and Technology*, vol. 29, no. 5, p. 19.
  - [21] Chen, Y, Wang, Y, Hu, F, Feng, L, Zhou, T & Zheng, C 2021, 'LDNNET: Towards Robust Classification of Lung Nodule and Cancer Using Lung Dense Neural Network', *IEEE Access*, vol. 9, pp. 50301-50320.
  - [22] Kweik, OMA, Hamid, MAA, Sheqlih, SO, Abu-Nasser, BS & Abu-Naser, SS 2020, 'Artificial Neural Network for Lung Cancer Detection', *International Journal of Academic Engineering Research (IJAER)*, vol. 4, no. 11.
  - [23] Nuyttens, J, Prévost, J-B, Praag, J, Hoogeman, M, Van Klaveren, R, Levendag, P & Pattynama, P 2006, 'Lung tumor tracking during stereotactic radiotherapy treatment with the CyberKnife: Marker placement and early results', *Acta Oncologica*, vol. 45, no. 7, pp. 961-965.
  - [24] Russo, A, De Miguel Perez, D, Gunasekaran, M, Scilla, K, Lapidus, R, Cooper, B, Mehra, R, Adamo, V, Malapelle, U & Rolfo, C 2019, 'Liquid biopsy tracking of lung tumor evolutions over time', *Expert review of molecular diagnostics*, vol. 19, no. 12, pp. 1099-1108.
  - [25] Sandhiya, S & Palani, U 2020, 'An effective disease prediction system using incremental feature selection and temporal convolutional neural network', *Journal of Ambient Intelligence and Humanized Computing*, vol. 11, no. 11, pp. 5547-5560.
  - [26] Priya, RM & Venkatesan, P 2021, 'An efficient image segmentation and classification of lung lesions in pet and CT image fusion using DTWT incorporated SVM', *Microprocessors and Microsystems*, vol. 82, p. 103958.
  - [27] Rebouças Filho, PP, da Silva Barros, AC, Ramalho, GL, Pereira, CR, Papa, JP, de Albuquerque, VHC & Tavares, JMR

- 2019, 'Automated recognition of lung diseases in CT images based on the optimum-path forest classifier', *Neural Computing and Applications*, vol. 31, no. 2, pp. 901-914.
- [28] Rossetto, AM & Zhou, W 2017, 'Deep learning for categorization of lung cancer ct images', in 2017 IEEE/ACM International Conference on Connected Health: Applications, Systems and Engineering Technologies (CHASE), pp. 272-273.
- [29] Wisely, CE, Wang, D, Henao, R, Grewal, DS, Thompson, AC, Robbins, CB, Yoon, SP, Soundararajan, S, Polascik, BW & Burke, JR 2020, 'Convolutional neural network to identify symptomatic Alzheimer's disease using multimodal retinal imaging', *British Journal of Ophthalmology*.
- [30] Xiaoming, S, Ning, Z, Haibin, W, Xiaoyang, Y, Xue, W & Shuang, Y 2018, 'Medical image retrieval approach by texture features fusion based on Hausdorff distance', *Mathematical Problems in Engineering* vol. 2018.
- [31] Ismaeel, N.Q., Mohammed, H.J., Chalob, I.Z. et al. Application of Healthcare Management Technologies for COVID-19 Pandemic Using Internet of Things and Machine Learning Algorithms. *Wireless Pers Commun* (2023). <https://doi.org/10.1007/s11277-023-10663-2>
- [32] Alhayani, B.A., AlKawak, O.A., Mahajan, H.B. et al. Design of Quantum Communication Protocols in Quantum Cryptography. *Wireless Pers Commun* (2023). <https://doi.org/10.1007/s11277-023-10587-x>
- [33] Omar A. AlKawak, Bilal A. Ozturk, Zinah S. Jabbar, Husam Jasim Mohammed, Quantum optics in visual sensors and adaptive optics by quantum vacillations of laser beams wave propagation apply in data mining, *Optik*, Vol,273,2023,170396, <https://doi.org/10.1016/j.ijleo.2022.170396>.